

Electronic Supplementary Information

Croconate Directed Supramolecular Self-Healable Cd(II)-Metallogel with Dispersed 2D-Nanosheets of Hexagonal Boron Nitride: A Comparative Outcome of Charge Transport Phenomena and Non-Linear Rectifying Behaviour of Semiconducting Diodes

Santanu Majumdar,^a Baisakhi Pal,^b Rajib Sahu,^c Krishna Sundar Das,^d Partha Pratim Ray,^{*,b} Biswajit Dey^{*,a}

^aDepartment of Chemistry, Visva-Bharati University, Santiniketan 731235, India.

^bDepartment of Physics, Jadavpur University, Kolkata-700032, India.

^cMax-Planck-Institut für Eisenforschung GmbH, Max-Planck-Str. 1, 40237 Düsseldorf, Germany.

^dSchool of Chemical Sciences, Indian Association for the Cultivation of Science, Jadavpur, Kolkata, West Bengal 700032

1. Minimum Critical Gelation Concentration (MGC) of Cd-CADS metallogel:

The minimum critical gel concentration (MGC) of Cd-CADS metallogel has been evaluated. The concentrations of gel-forming chemical-ingredients i.e. $\text{Cd}(\text{CH}_3\text{COO})_2 \cdot 2\text{H}_2\text{O}$ and croconic acid disodium salt (CADS) were maintained as 1:1, w/w. Following this stoichiometric aspect, the concentration of metal salt and organic gelator were varied in the span of 50-565 mg mL^{-1} (See the Fig S1 where different concentrations are noted). The best quality gel of the supramolecular Cd-CADS metallogel was appeared when the concentration of Cd(II)-salt and croconic acid disodium salt were taken as 565 mg mL^{-1} . Fig. S1 shows the concentrations of gel-forming chemicals taken as 50, 150, 350, 450, 500, 565 mg mL^{-1} , designated by (a), (b), (c), (d), (e), and (f), respectively.

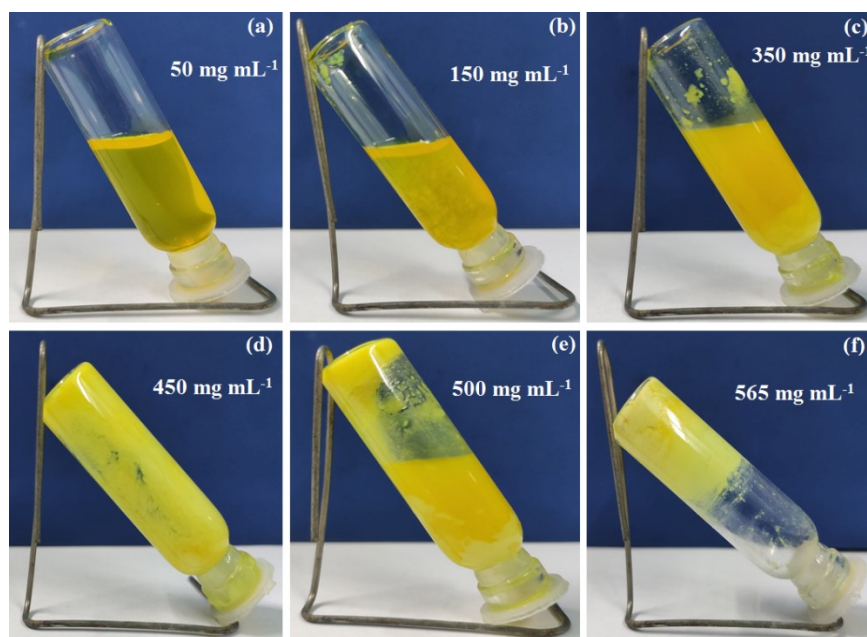


Fig. S1. Investigation of minimum critical gelation concentration (MGC) of Cd-CADS metallogel.

2. Rheological Studies of Cd-CADS metallogel:

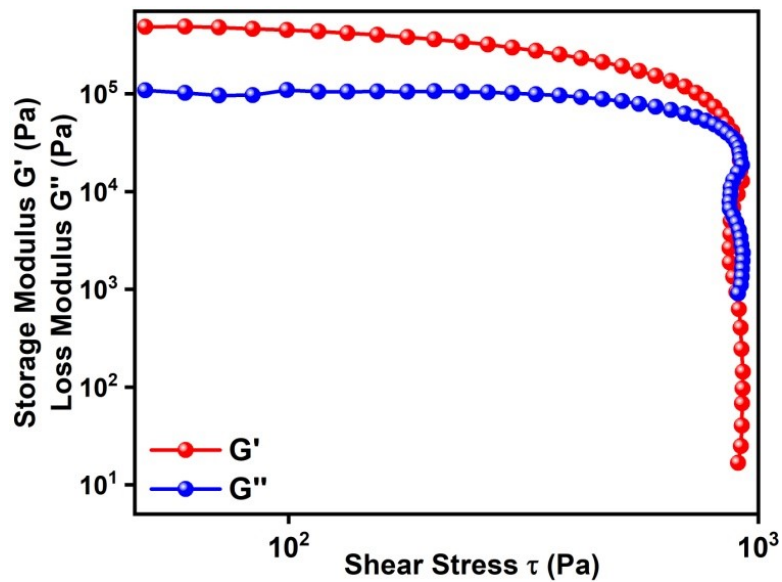


Fig. S2. Stress sweep of Cd-CADS metallogel.

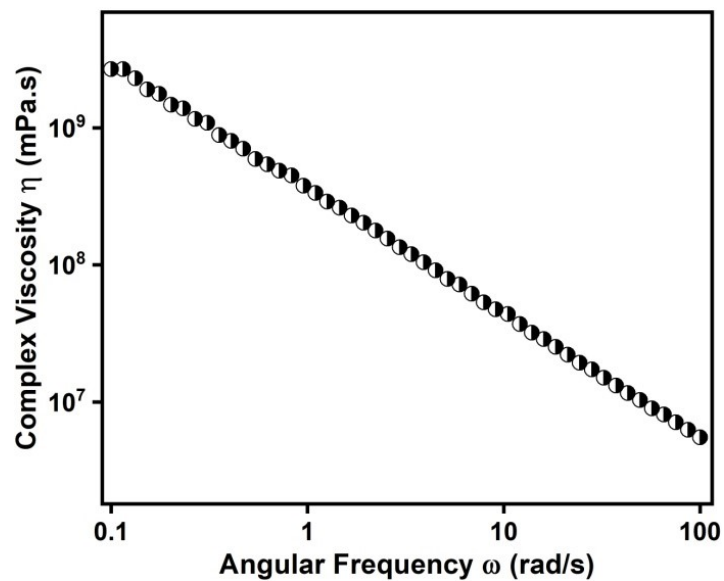


Fig. S3. Complex viscosity vs. angular frequency plot of Cd-CADS metallogel.

3. Visualization of Self-Healing properties of Cd-CADS metallogel:

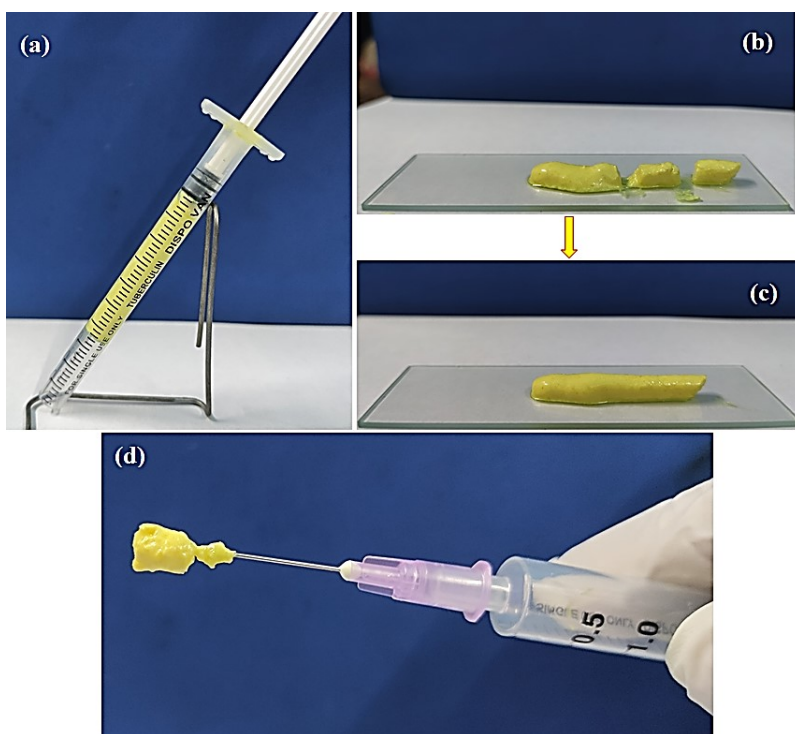


Fig. S4. Self-Healing property of Cd-CADS metallogel: (a) Inverted image of the Cd-CADS metallogel; (b) cutting the gel into pieces and (c) regeneration after self-healing; (d) shows that the Cd-CADS metallogel can sustain in a mouth of a pin which ratifies the exceptional stability of the metallogel.

Microstructural Studies

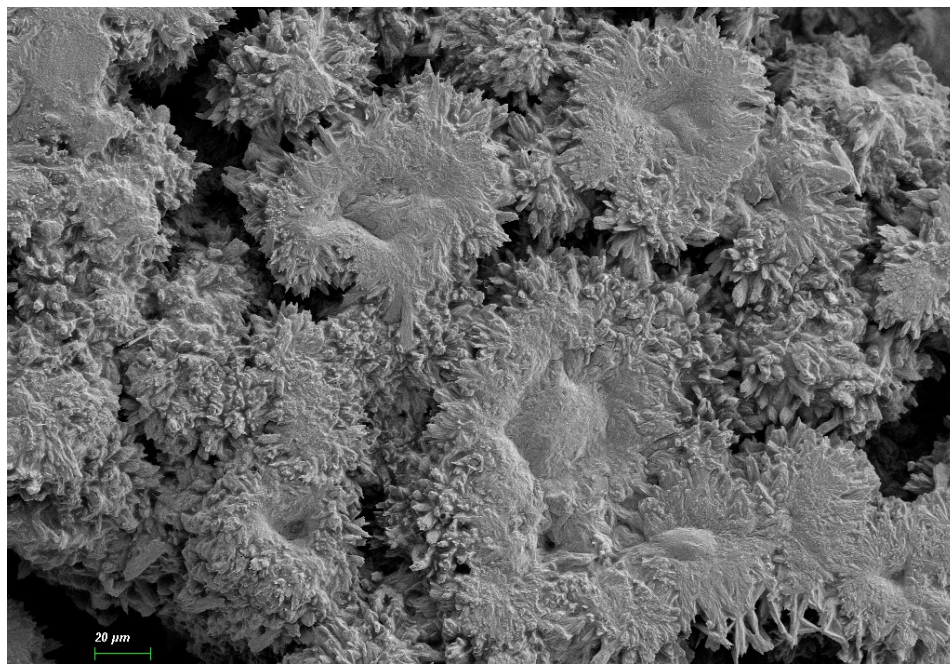


Fig. S5. Hierarchical type stacked-flower like FESEM microstructural pattern of Cd-CADS xerogel.

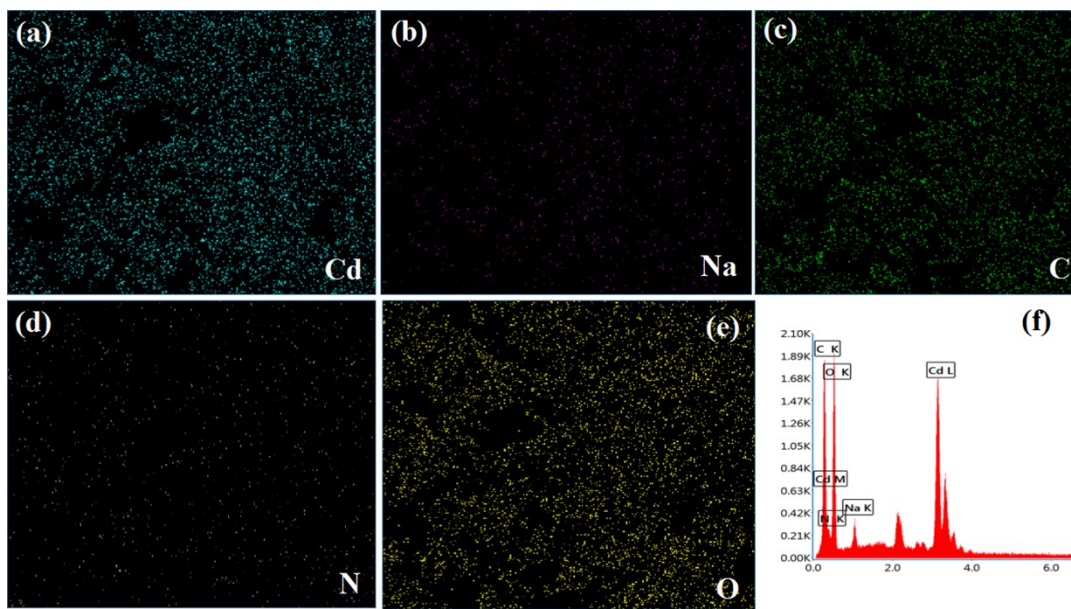


Fig. S6. (a-e) EDX pattern of Cd-CADS xerogel shows Cadmium, Sodium, Carbon, Nitrogen, and Oxygen elements of Cd-CADS scaffold, (f) EDS elemental spectrum of Cd-CADS xerogel.

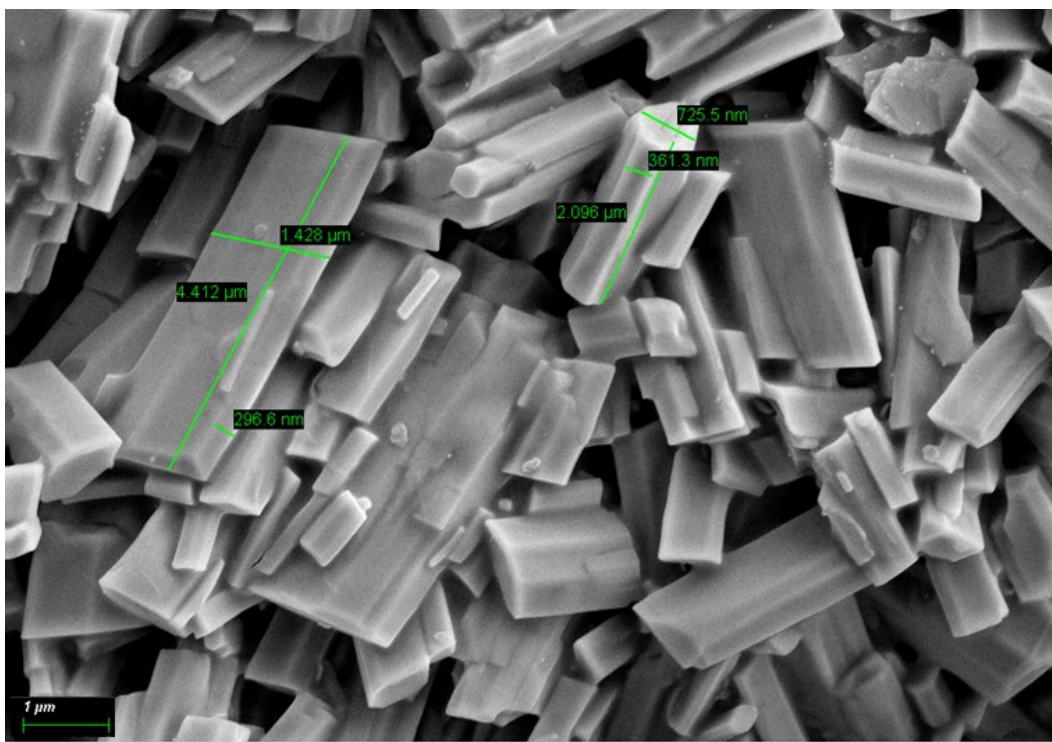


Fig. S7. Hexagonal rod type FESEM microstructural pattern of h-BN@Cd-CADS xerogel.

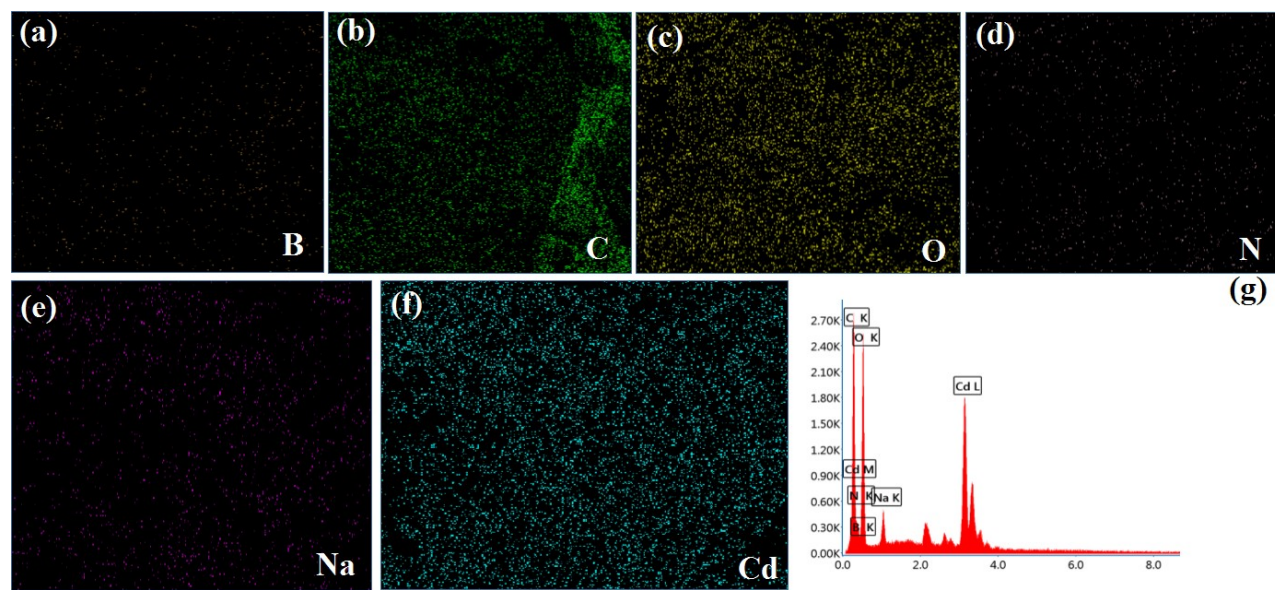


Fig. S8. (a-f) EDX pattern of h-BN@Cd-CADS xerogel shows Boron, Carbon, Oxygen Nitrogen, Sodium and Cadmium, elements of h-BN@Cd-CADS scaffold, (g) EDS elemental spectrum of h-BN@Cd-CADS xerogel.

Electrical Property Analysis

Thermionic Emission theory:

According to Thermionic Emission theory, the forward bias current density can be expressed as

$$J = J_0 \left[\exp\left(\frac{qV}{\eta K T}\right) - 1 \right] \quad (1)$$

When $V=0$, $J=J_0$ =Saturation Current Density = $A^* T^2 \exp\left(-\frac{q\Phi_B}{KT}\right)$ (2)

Where, q =Electronic Charge, V =Applied Voltage, η = Ideality Factor, K =Boltzman's Constant, T =Temperature in Kelvin scale, Φ_B = Barrier potential Height, A^* = Recharldson's constant and was considered as $1.2 \times 10^6 \text{ A m}^{-2} \text{ K}^{-2}$.

Cheung's method:

According to Cheung's model, when a series resistance is designed as a series combination of resistor and diode, then the voltage across the diode can be substituted as the voltage drop across the series combination of diode and resistor. Then equation (1) can be drafted as,

$$J = J_0 \left[\exp\left(\frac{q(V - I R_S)}{\eta K T}\right) \right] \quad (3)$$

Where, IR_S term indicates the voltage drop across the series resistance of the semiconductor diode. Inserting the value of saturation current density into equation (3), and differentiate with respect to $\ln J$, we get,

$$\frac{dV}{d \ln J} = A J R_S + \frac{\eta K T}{q} \quad (4)$$

Where, R_S =series resistance, q =Electronic Charge, η = Ideality Factor, K =Boltzman's Constant, T =Temperature in Kelvin scale

As stated in the Cheung model, the current density-reliant function $H(J)$ can be written as,

$$H(J) = V - \frac{\eta K T}{q} \ln \left(\frac{J}{A^* T^2} \right) = A J R_S + \eta \Phi_B \quad (5)$$

Where, Φ_B = Barrier height, A^* = Recharadson's constant and was considered as $1.2 \times 10^6 \text{ A m}^{-2} \text{ K}^{-2}$

Mott-Gurney equation:

Taking the slope of the J vs. V^2 graphs of region II, the effective interface mobility (μ_{eff}) of the charge carrier was estimated using Mott-Gurney space charge limited current density

$$J = \frac{9 \mu_{eff} \epsilon_0 \epsilon_r}{8} \left(\frac{V^2}{d^3} \right) \quad (6)$$

ϵ_0 and ϵ_r is the dielectric permittivity of vacuum and dielectric constant of synthesized film respectively measured from capacitance(C)-frequency (f) curve shown in Fig. S6. The relative dielectric constant of Cd-CADS metallogel based device was calculated to be 5.063 and of BN@Cd-CADS was 20.52.

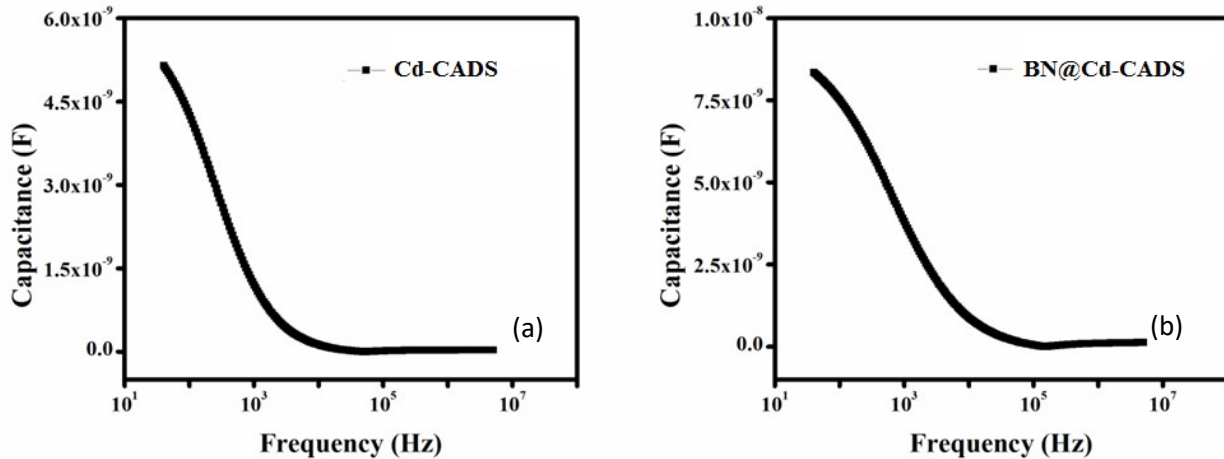


Fig. S9. Capacitance versus frequency plot (a) Cd-CADS (b) h-BN@Cd-CADS metallogel based devices

From the saturation level of the curve of the Fig. S5 (a) and (b) the dielectric permittivity of the semiconductor was evaluated by using equation,

$$\epsilon_r = \frac{1 C_{sat} d}{\epsilon_0 A} \quad (7)$$

Where d is the film thickness and A is the area of the diode.

$$\tau = \frac{9 \epsilon_0 \epsilon_r (V)}{8 d (J)} \quad (8)$$

The charge carrier concentration (N) was calculated using formula,

$$N = \frac{\sigma_{SCLC}}{q \mu_{eff}}$$

(9)

the SCLC region conductivity.

Where, σ_{SCLC} is